Available online at www.sciencedirect.com

SCIENCE DIRECT®

Inorganica Chimica Acta 359 (2006) 585–592

Inorganica Chimica Acta

www.elsevier.com/locate/ica

Synthesis, spectroscopic and redox properties of some ruthenium(II) thiosemicarbazone complexes: Structural description of four of these complexes

Dipankar Mishra [a], Subhendu Naskar [a], Michael G.B. Drew [b], Shyamal Kumar Chattopadhyay [a,*]

[a] *Department of Chemistry, Bengal Engineering and Science University, Shibpur College Road, P.O. Botanic Garden, Howrah 711 103, West Bengal, India*
[b] *School of Chemistry, University of Reading, Whiteknights, Reading RG6 6AD, UK*

Received 7 July 2005; received in revised form 24 October 2005; accepted 3 November 2005
Available online 13 December 2005

Abstract

Sixteen neutral mixed ligand thiosemicarbazone complexes of ruthenium having general formula $[Ru(PPh_3)_2L_2]$, where LH = 1-(arylidine)4-aryl thiosemicarbazones, have been synthesized and characterized. All complexes are diamagnetic and hence ruthenium is in the +2 oxidation state (low-spin d^6, $S = 0$). The complexes show several intense peaks in the visible region due to allowed metal to ligand charge transfer transitions. The structures of four of the complexes have been determined by single-crystal X-ray diffraction and they show that thiosemicarbazone ligands coordinate to the ruthenium center through the hydrazinic nitrogen and sulfur forming four-membered chelate rings with ruthenium in $N_2S_2P_2$ coordination environment. In dichloromethane solution, the complexes show two quasi-reversible oxidative responses corresponding to loss of electron from HOMO and HOMO − 1. The E^0 values of the above two oxidations shows good linear relationship with Hammett substituents constant (σ) as well as with the HOMO energy of the molecules calculated by the EHMO method. A DFT calculation on one representative complex suggests that there is appreciable contribution of the sulfur p-orbitals to the HOMO and HOMO − 1. Thus, assignment of the oxidation state of the metal in such complexes must be made with caution.

Keywords: Ruthenium(II) thiosemicarbazone complexes; Synthesis; X-ray structures; Cyclic voltammetry; Oxidation; EHMO calculations; DFT calculations; Hammett correlation

1. Introduction

Thiosemicarbazones are an important class of N, S donor ligand which have considerable pharmacological interest due to their significant antibacterial, antiviral, antimalarial, antileprotic and anticancer activities [1–6]. Several metal complexes of thiosemicarbazones particularly with copper, platinum, palladium, rhenium and ruthenium also show marked and diverse biological activity [7–12]. The chemistry of complexes of ruthenium with thiosemicarbazones, which can coordinate to the metal either in neutral thione form or in the anionic thiolate form, has received attention in recent years primarily due to their varied coordination mode, novel electrochemical and electronic properties [13–19], as well as their biological importance [13,14,20–23].

In this study, we report the synthesis, characterization, spectroscopic and redox behaviors of 16 ruthenium (II) complexes of 1-(arylidine) 4-(aryl) thiosemicarbazones obtained by condensation of 4-(aryl) thiosemicarbazides with *para* substituted benzaldehyde. X-ray crystal structures of four such complexes are also reported here.

---

[*] Corresponding author. Fax: +91 33 2668 2916.
E-mail address: shch20@hotmail.com (S.K. Chattopadhyay).

0020-1693/$ - see front matter © 2005 Elsevier B.V. All rights reserved.
doi:10.1016/j.ica.2005.11.001

2. Experimental

$Ru(PPh_3)_3Cl_2$ was prepared by the published procedure [24]. Analytical, magnetic, spectroscopic and electrochemical data were acquired as described in our earlier papers [25,26].

2.1. Synthesis of the ligands

The ligands (Scheme 1), 4-(phenyl)thiosemicarbazones of benzaldehyde (L^1H) (**1**), anisic aldehyde (L^2H) (**2**), *p*-chlorobenzaldehyde (L^3H) (**3**), *p*-*N*,*N*-dimethyl aminobenzaldehyde (L^4H) (**4**), 4-(*p*-methylphenyl)thiosemicarbazones of (**5**) benzaldehyde (L^5H) (**5**), anisic aldehyde (L^6H) (**6**), *p*-chlorobenzaldehyde (L^7H) (**7**), *p*-*N*,*N*-dimethyl aminobenzaldehyde (L^8H) (**8**), 4-(*p*-chlorophenyl)thiosemicarbazones of (**9**) benzaldehyde (L^9H) (**9**), anisic aldehyde ($L^{10}H$) (**10**), *p*-chlorobenzaldehyde ($L^{11}H$) (**11**), *p*-*N*,*N*-dimethyl aminobenzaldehyde ($L^{12}H$) (**12**), 4-(*p*-fluorophenyl)thiosemicarbazones of (**13**) benzaldehyde ($L^{13}H$) (**13**), anisic aldehyde ($L^{14}H$) (**14**), *p*-chlorobenzaldehyde ($L^{15}H$) (**15**), *p*-*N*,*N*-dimethyl aminobenzaldehyde ($L^{16}H$) (**16**) were prepared using the corresponding amines by the published procedure [13,14].

2.2. Synthesis of the complexes

All the complexes (**1–16**) of general formulae $[Ru(PPh_3)_2(L)_2]$ (where L represents the deprotonated ligand) were synthesized following a common procedure with almost similar yields. Therefore, synthetic details of just one representative example is given below:

To a 30 ml methanolic solution of the L^2H (142.5 mg, 0.5 mmol), Et_3N (50 mg, 0.5 mol) was added, followed by the addition of solid $[Ru(PPh_3)_3Cl_2]$ (240 mg, 0.25 mmol). After 3 h of reflux the shiny yellow precipitate that separated out during reflux was collected by filtration and washed thoroughly with cold methanol. Recrystallisation of the product from 1:1 dichloromethane–methanol solution leads to golden yellow crystals. Yield: 75–80%.

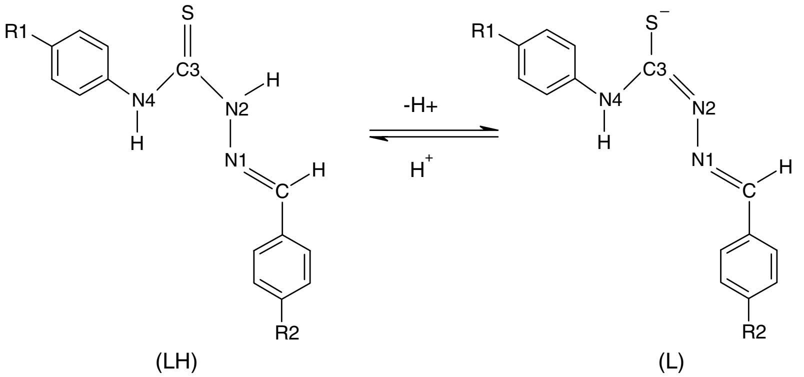

R1	R2	LH
H	H	L^1H
H	OMe	L^2H
H	Cl	L^3H
H	NMe_2	L^4H
CH_3	H	L^5H
CH_3	OMe	L^6H
CH_3	Cl	L^7H
CH_3	NMe_2	L^8H
Cl	H	L^9H
Cl	OMe	$L^{10}H$
Cl	Cl	$L^{11}H$
Cl	NMe_2	$L^{12}H$
F	H	$L^{13}H$
F	OMe	$L^{14}H$
F	Cl	$L^{15}H$
F	NMe_2	$L^{16}H$

Scheme 1.

Anal. Calc. for $C_{64}H_{54}N_6P_2S_2Ru$ (**1**): C, 67.78; H, 4.76; N, 7.41. Found: C, 67.81; H, 4.80; N, 7.42%. *Anal.* Calc. for $C_{67}H_{61}ClN_6O_{2.5}P_2S_2$ Ru (**2**): C, 64.24; H, 4.87; N, 6.71. Found: C, 64.29; H, 4.90; N, 6.73%. *Anal.* Calc. for $C_{60}H_{52}ClN_6P_2S_2Ru$ (**3**): C, 59.90; H, 4.32; N, 6.98. Found: C, 59.98; H, 4.36; N, 6.94%. *Anal.* Calc. for $C_{68}H_{64}N_8P_2S_2Ru$ (**4**): C, 66.94; H, 5.25; N, 9.18. Found: C, 67.02; H, 5.29; N, 9.13%. *Anal.* Calc. for $C_{66}H_{59}N_6O_{0.5}P_2S_2Ru$ (**5**): C, 67.69; H, 5.04; N, 7.17. Found: C, 67.72; H, 5.08; N, 7.20%. *Anal.* Calc. for $C_{68.5}H_{62}N_6O_3P_2S_2Ru$ (**6**): C, 65.97; H, 5.21; N, 6.74. Found: C, 66.01; H, 5.24; N, 6.76%. *Anal.* Calc. for $C_{66}H_{56}Cl_2N_6P_2S_2Ru$ (**7**): C, 64.39; H, 4.55; N, 6.82. Found: C, 64.45; H, 4.60; N, 6.77%. *Anal.* Calc. for $C_{70}H_{68}N_8P_2S_2Ru$ (**8**): C, 67.39; H, 5.45; N, 8.98. Found: C, 67.42; H, 5.47; N, 8.92%. *Anal.* Calc. for $C_{64}H_{52}Cl_2N_6P_2S_2Ru$ (**9**): C, 63.89; H, 4.32; N, 6.98. Found: C, 63.97; H, 4.35; N, 6.92%. *Anal.* Calc. for $C_{67}H_{57}Cl_3N_6O_2P_2S_2Ru$ (**10**): C, 61.36; H, 4.36; N, 6.43. Found: C, 61.69; H, 4.37; N, 6.45%. *Anal.* Calc. for $C_{64}H_{50}Cl_4N_6P_2S_2Ru$ (**11**): C, 60.42; H, 3.93; N, 6.60. Found: C, 60.49; H, 3.97; N, 6.54%. *Anal.* Calc. for $C_{68}H_{62}Cl_2N_8P_2S_2Ru$ (**12**): C, 63.35; H, 4.81; N, 8.69. Found: C, 63.42; H, 4.85; N, 8.58%. *Anal.* Calc. for $C_{64}H_{52}F_2N_6P_2S_2$ Ru (**13**): C, 65.69; H, 4.44; N, 7.18. Found: C, 65.76; H, 4.47; N, 7.09%. *Anal.* Calc. for $C_{66}H_{56}F_2N_6O_2P_2S_2Ru$ (**14**): C, 64.44; H, 4.55; N, 6.83. Found: C, 64.52; H, 4.59; N, 6.78%. *Anal.* Calc. for $C_{64}H_{50}Cl_2F_2N_6P_2S_2Ru$ (**15**): C, 62.03; H, 4.03; N, 6.78. Found: C, 62.11; H, 4.09; N, 6.69%. *Anal.* Calc. for $C_{68}H_{62}F_2N_8P_2S_2Ru$ (**16**): C, 65.01; H, 4.94; N, 8.92. Found: C, 65.12; H, 4.97; N, 8.87%.

2.3. Computational chemistry

EHMO calculations were carried out on the MM^+ optimized structures of the complexes using the Window based Hyperchem program [27]. For both MM^+ and EHMO calculations, the default parameters of the program were used. A DFT calculation on one of the complexes (**1**) was performed using the ADF program [28]. Geometry optimization for the DFT calculation was carried out using the default criteria for convergence in the ADF program. For all elements the ZORA approximation was used together with the default TZP basis sets using a small core. In addition Vosko, Wilk and Nusair's local exchange correlation potential was used [29] together with Becke's non-local exchange [30] and Perdew's correlation corrections [31].

2.4. X-ray crystallography

Single crystals for **2** and **6** were grown from slow evaporation of dichloromethane–methanol solution and those of **5** and **10** were obtained from dichloromethane–acetonitrile solution of the complexes. Data were measured with Mo Kα radiation using the MAR research Image Plate System at 293 K. The crystals were positioned at 70 mm from the Image Plate. One hundred frames were measured at 2° intervals with a counting time of 2 min. Data analysis was carried out with the XDS program [32]. The structures were solved using direct methods with the SHELX-86 program [33]. Non-hydrogen atoms were refined with anisotropic thermal parameters. The hydrogen atoms bonded to carbon were included in geometric positions and given thermal parameters equivalent to 1.2 times those of the atom to which they were attached. Empirical absorption corrections were applied using DIFABS [34]. The structures were refined on F^2 using SHELXL [35]. CCDC numbers of the structures are 265804, 265805, 265807 and 265806 for complexes **2**, **5**, **6** and **10**, respectively.

2.5. Description of the crystal structures

Structures **2**, **6** and **10** are isomorphous, while **5** is not isomorphous. The molecular structures (Figs. 1–4) are very similar in that the metal atom occupies a six-coordinate octahedral environment with the metal bonded to two triphenylphosphine ligands and two bidentate deprotonated thiosemicarbazone ligands (L) forming four membered chelate rings through thiolato sulfur and nitrogen (N2). The two triphenylphosphine ligands are mutually *cis* with angles significantly greater than 90°, ranging from 96.6(10) to 98.1(1)°, no doubt because of the bulky nature of the ligand. The Ru–P bond lengths range from 2.292(6)–2.323(4) Å. The bidentate ligands show small bite angles, thus the N–Ru–S angles range from 65.1(2) to 66.0(2)°. In the structures, the sulfur atoms are mutually *trans*, but the nitrogen atoms are *cis* to each other. The Ru–S distances range from 2.428(3) to 2.452(3) Å, and the Ru–N distances from 2.132(11)–2.183(10) Å. All the observations are comparable to the values reported earlier [15–19,26]. It may be noted that among the four structures reported here,

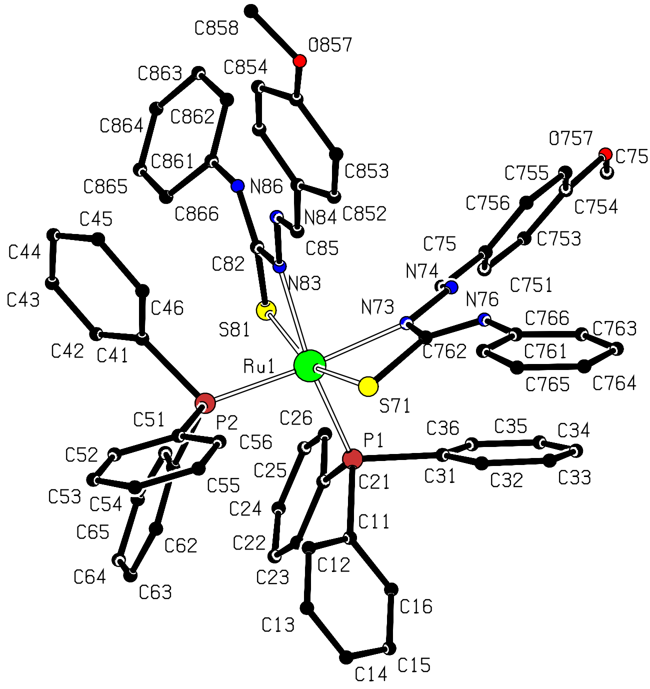

Fig. 1. X-ray crystal structure of **2**.

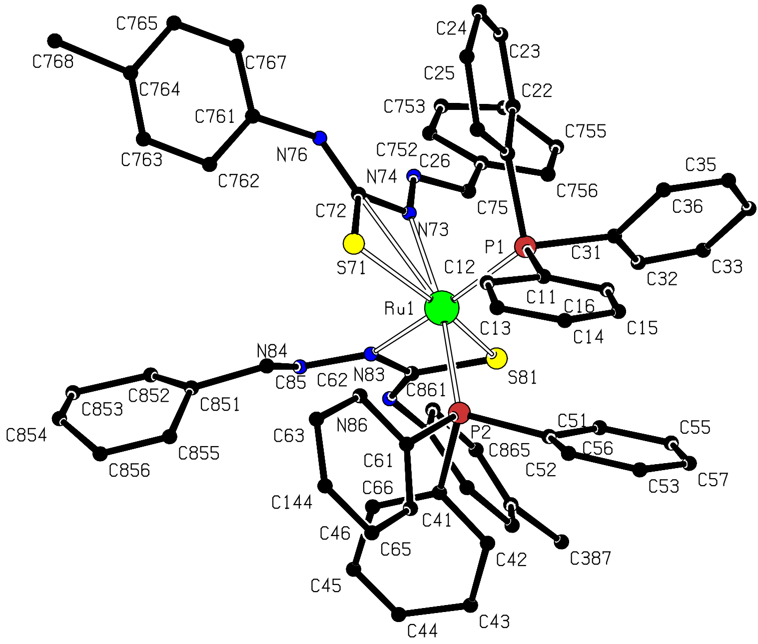

Fig. 2. X-ray crystal structure of **5**.

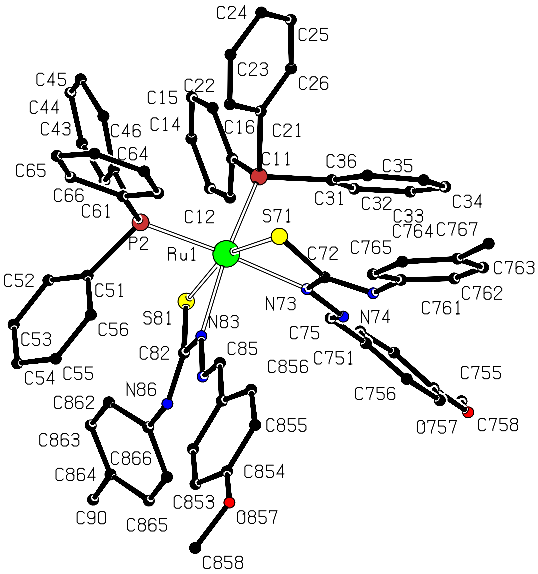

Fig. 3. X-ray crystal structure of **6**.

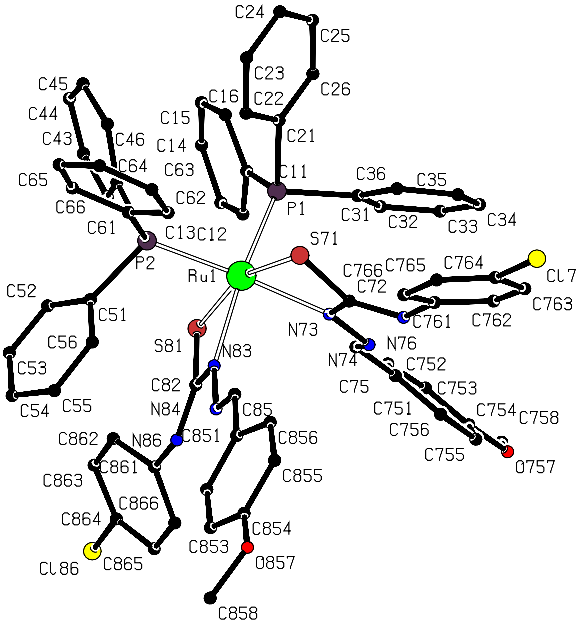

Fig. 4. X-ray crystal structure of **10**.

while the Ru–P and Ru–S bond distances are not so sensitive to the variation at R1 (H, Me, Me and Cl for **2**, **5**, **6**, **10**, respectively) and R2 (OMe for **2**, **6** and **10**, H for **5**), the Ru–N bond is found to be appreciably shorter in **5** (average = 2.137 Å, R2 = H) compared to the other three structures (average values are 2.179, 2.176, 2.164 Å for **2**, **6** and **10**, respectively; R2 = OMe). Between **2**, **6** and **10** the average Ru–N, Ru–P distances are all shorter in **10** (R1 = Cl, average Ru–N, Ru–P distances are 2.164, 2.305 Å, respectively) compared to **2** (R1 = H, Ru–N, Ru–P distances are 2.179, 2.316 Å, respectively) and **6** (R1 = Me, Ru–N, Ru–P distances are 2.176, 2.310 Å, respectively). It may be noted that due to the formation of the four-membered chelate rings the carbon atom of the thiosemicarbazone moiety (C72 and C82) is at appreciably short distance from the ruthenium (Ru–C72/C82 distances lie within a range of 2.71–2.82 Å, which may be compared with sum of the covalent radii of Ru and C (2.33 Å) and sum of their van der Waal's radii (4.00 Å)). In fact the Ru–C72 distance (2.71(2) Å) in compound **5** is so short that it may be considered as pseudo-seven coordinated species. Moreover, there are also several Ru ⋯ H short contacts (see supplementary table ST1), particularly involving the H atoms attached to aldimine moieties

(H75 and H85). These Ru ⋯ H–C hydrogen bonds along with some additional Ru ⋯ H interactions involving phenyl protons of the PPh_3 ligand and the N76–H76 ⋯ N74 and N86–H86 ⋯ N84 hydrogen bonds probably contribute towards stabilizing the four membered chelate rings in these complexes. The details list of hydrogen bonds for the compounds **2**, **5**, **6** and **10** are given in supplementary tables ST2, ST3, ST4 and ST5, respectively.

3. Results and discussion

3.1. Synthesis and some properties

A series of ruthenium complexes using 4-(aryl) thiosemicarbazones of aromatic aldehydes (LH) as ligands of general formulae $[Ru(PPh_3)_2(L)_2]$ (**1**–**16**) have been synthesized. Detailed synthetic methods have been described above. The elemental analyses, molar conductivity data, room temperature magnetic moment and spectroscopic data are consistent with their respective formulae as stated above (see Tables 1 and 2).

3.2. Electronic spectra

Electronic spectra were recorded in dichloromethane solution and data are displayed in Table 3. Each complex shows intense absorption in the visible region that is probably due to the allowed MLCT transitions as is generally observed in low spin d^6 ruthenium complexes [36–38]. Multiple charge transfer transitions in such mixed ligand complexes may result from splitting of metal orbitals in lower symmetry and presence of different acceptor levels in the ligands. All other transitions in the UV region are assigned to intra ligand transitions.

3.3. Electrochemistry

Electron transfer properties of the complexes were examined by cyclic voltammetry in dichloromethane (in the presence of 0.1 M tetraethylammonium perchlorate (TEAP)) solution and results are presented in Table 3. All the complexes show two oxidative responses on the positive side of Ag/AgCl reference electrode. One selected voltammogram is shown in Fig. 5. This first oxidation is quasi reversible, with a peak-to-peak separation of 76–123 mV as evident from cyclic voltammetric data, and the anodic peak current (i_{pa}) is almost equal to the cathodic peak current (i_{pc}). The one-electron nature of this oxidation has been tentatively established by comparing its current height with that of standard ferrocene/ferrocenium couple under the same experimental condition. The complexes show a second oxidative response at the potential range 0.77–1.25 V. The earlier authors [16,17] have assigned these two oxidations to Ru^{II}/Ru^{III} and

Table 2
Bond distances (Å) and bond angles (°) for complexes **2**, **5**, **6** and **10**

	2	5	6	10
Ru(1)–N(83)	2.173(9)	2.132(11)	2.173(6)	2.168(7)
Ru(1)–N(73)	2.183(10)	2.143(14)	2.178(6)	2.165(7)
Ru(1)–P(1)	2.309(4)	2.315(5)	2.308(3)	2.299(3)
Ru(1)–P(2)	2.323(4)	2.292(6)	2.313(3)	2.312(3)
Ru(1)–S(81)	2.452(3)	2.432(4)	2.431(3)	2.433(3)
Ru(1)–S(71)	2.443(4)	2.441(5)	2.424(3)	2.428(3)
N(83)–Ru(1)–N(73)	82.7(5)	83.3(5)	83.7(2)	83.6(2)
N(83)–Ru(1)–P(1)	164.1(2)	169.8(3)	165.1(2)	165.5(2)
N(83)–Ru(1)–P(2)	90.4(2)	91.2(4)	90.8(2)	91.0(2)
N(83)–Ru(1)–S(81)	65.5(2)	65.6(3)	65.9(2)	65.9(2)
N(83)–Ru(1)–S(71)	99.7(3)	95.8(3)	98.8(2)	99.0(2)
N(73)–Ru(1)–P(1)	90.4(2)	89.5(3)	90.0(2)	90.3(2)
N(73)–Ru(1)–P(2)	167.5(2)	171.5(3)	168.6(2)	168.6(2)
N(73)–Ru(1)–S(81)	100.6(3)	96.5(3)	99.4(2)	99.8(2)
N(73)–Ru(1)–S(71)	65.1(3)	65.7(3)	65.9(2)	65.6(2)
P(1)–Ru(1)–P(2)	98.1(1)	96.7(2)	97.6(10)	97.2(1)
P(1)–Ru(1)–S(81)	102.1(1)	108.3(2)	102.1(1)	102.5(1)
P(1)–Ru(1)–S(71)	90.2(1)	87.8(2)	90.9(1)	90.4(1)
P(2)–Ru(1)–S(81)	86.6(1)	87.1(2)	87.3(1)	87.0(1)
P(2)–Ru(1)–S(71)	105.5(1)	108.5(2)	105.3(1)	105.6(1)
S(71)–Ru(1)–S(81)	161.5(1)	156.4(2)	160.7(1)	160.9(1)

Table 1
Crystallographic data for **2**, **5**, **6** and **10**

Complex	2	5	6	10
Empirical formula	$C_{67}H_{61}ClN_6O_{2.5}P_2RuS_2$	$C_{66}H_{59}N_6O_{0.5}P_2RuS_2$	$C_{68.5}H_{65}N_6O_3P_2RuS_2$	$C_{67}H_{57}Cl_3N_6O_2P_2Ru$
Formula weight	1251.82	1171.31	1247.39	1304.68
Crystal system, space group	monoclinic, $P2_1/c$	monoclinic, $P2_1/n$	monoclinic, $P2_1/c$	monoclinic, $P2_1/c$
Unit cell dimensions				
a (Å)	12.660(14)	11.822(14)	12.555(14)	12.498(14)
b (Å)	23.800(27)	40.108(45)	23.362(25)	23.299(25)
c (Å)	21.765(24)	12.371(14)	22.513(25)	22.412(24)
β (°)	105.54(1)	92.48(1)	101.70(1)	101.43(1)
Volume (Å^3)	6322.6	5860.3	6466.1	6396.7
Z, calculated density (Mg m^{-3})	4, 1.330	4, 1.333	4, 1.280	4, 1.364
Absorption coefficient (mm^{-1})	0.457	0.441	0.406	0.535
Unique reflections collected	10180	4094	9720	9031
Restraints/parameters	0/730	0/330	3/753	3/749
Final R indices $[1 > 2\sigma(I)]$ R_1, wR_2	0.1201, 0.2013	0.0978, 0.2781	0.0769, 0.2024	0.0796, 0.1987
R indices (all data)	0.1961, 0.2746	0.1641, 0.3003	0.1554, 0.2318	0.1841, 0.2313
Largest difference in peak and hole (e Å^{-3})	0.869, −0.704	0.749, −0.820	1.168, −1.124	0.903, −0.913

Table 3
Electronic spectral and cyclic voltammetric data

Complexes	Electronic spectral data[c] in CH_2Cl_2, λ_{max}/nm (ε/l mol^{-1} cm^{-1})	E^0/V (ΔE_p/mV) in CH_2Cl_2		
		$E_1^{0\ \dagger}$	$E_2^{0\ \dagger}$	E_3^0
1	431[a](6178), 340 (20758), 265[a](43247), 227 (78586)	0.51 (107)	1.25 (238)	
2	421[a](8334), 335 (22782), 243 (33756), 228 (48620)	0.47 (110)	1.05 (236)	
3	420[a] (20397), 344 (33146), 285[a] (53543), 228 (101987)	0.53(106)	1.20 (76)	
4	379 (13497), 277[a](9508),262[a](10439), 228 (20280)	0.34 (89)	0.77 (165)	1.14 (107)
5	410[a] (15085), 344 (22930) 271[a] (41033), 225 (70902)	0.47 (88)	1.15 (120)	
6	400[a] (21060), 348 (28258) 262 (53317), 227 (79975)	0.43(110)	1.10 (144)	
7	412[a] (13972), 352 (18663), 275[a] (32735), 240 (55091)	0.50 (91)	1.15 (120)	
8	418[a] (15757), 365 (19069), 273[a] (18667), 235 (40146)	0.33 (96)	0.77 (190)	1.12 (110)
9	412[a] (15018), 337 (26314), 287[a] (49674), 227 (84094)	0.52 (95)	1.17 (146)	
10	406[a] (15339), 341 (26295), 264 (45535), 227 (66725)	0.47(85)	1.07 (106)	
11	418 (16581), 341 (28634), 287[a](44641), 227 (84687)	0.55 (123)	1.17 (146)	
12	378 (87446), 270[a] (57212), 263[a] (61612), 227 (126713)	0.40 (76)	0.78 (128)	1.17 (82)
13	408[a] (15339), 337 (23711), 269[a] (45416), 227 (82932)	0.51 (94)	1.22 (135)	
14	406[a] (19380), 337 (30847), 262 (57333), 227 (87498)	0.46 (95)	1.08 (104)	
15	405 (17047), 343 (26295), 272[a] (46705), 227 (83361)	0.54 (101)	1.12 (214)	
16	376 (55411), 264[a] (43797), 227 (98543)	0.38(76)	0.77 (156)	1.14 (113)

† E_0^1 and E_0^2 are tentatively Ru^{III}/Ru^{II} and Ru^{IV}/Ru^{III} couples. However, due to appreciable admixture of sulfur orbitals with HOMO and HOMO − 1 the oxidation state of the metal cannot be defined unequivocally.

[a] Shoulder.

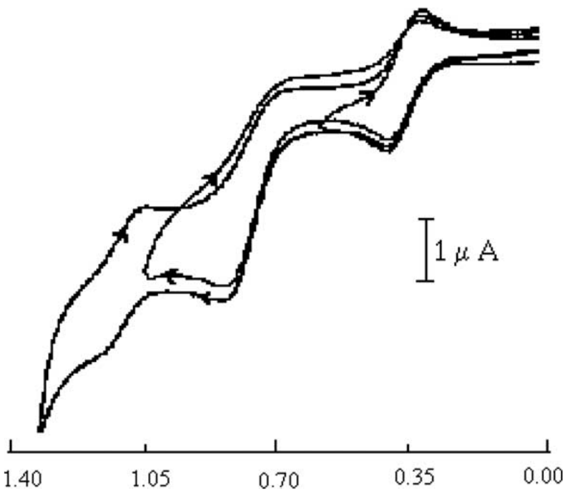

Fig. 5. Cyclic voltammogram of **4** in CH_2Cl_2.

Table 4
Results of DFT calculation on **1**

	Energy (a.u.)	% Atomic orbital coefficients
LUMO	−0.095649	No metal contribution
HOMO	−0.159906	31.6 Ru d_{xy}, 14.4 S p_y, 5.1 S p_z
HOMO − 1	−0.166758	50.6 Ru d_{xz}, 12.7 S p_x, 5.0 S p_z
HOMO − 2	−0.170253	20.1 Ru d_z^2, 17.7 d_{xy}, 9.8 S p_y
HOMO − 3	−0.175612	No metal contribution

Ru^{III}/Ru^{IV}, respectively. However, DFT calculation carried out on a representative molecule (**1**) shows (Table 4), that the HOMO has ~30% metal character and ~20% contributions from the sulfur orbitals. Thus, assignment of the oxidation state of the metal ion for such molecules must be made with caution as the electron is lost from a molecular orbital having appreciable ligand contribution rather than from a pure metal centered orbital.

In addition, complexes **4**, **8**, **12** and **16** also show a third quasi-reversible oxidative response at the potential range 1.12–1.17 V, which is tentatively assigned as ligand centered oxidation.

For all the complexes, the E_0^1 and E_0^2 values are found to be sensitive to the substituents (R1 and R2) on the aro-

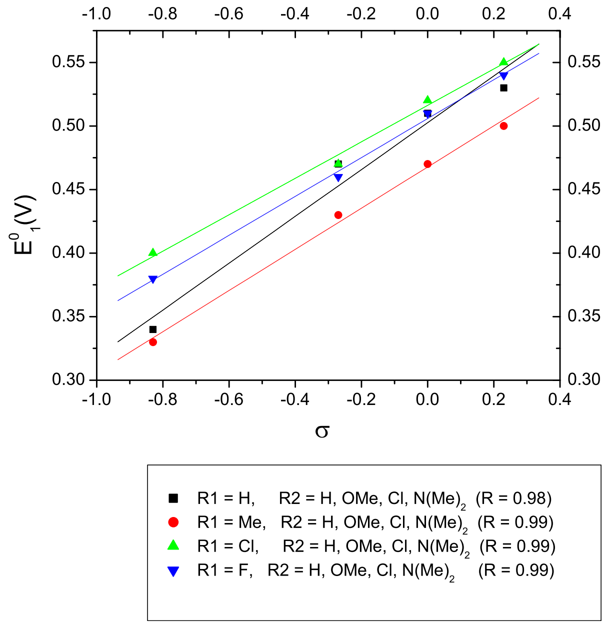

Fig. 6. Plot of E_0^1 (V) vs. Hammett substituents constant (σ) of R2 for a fixed R1.

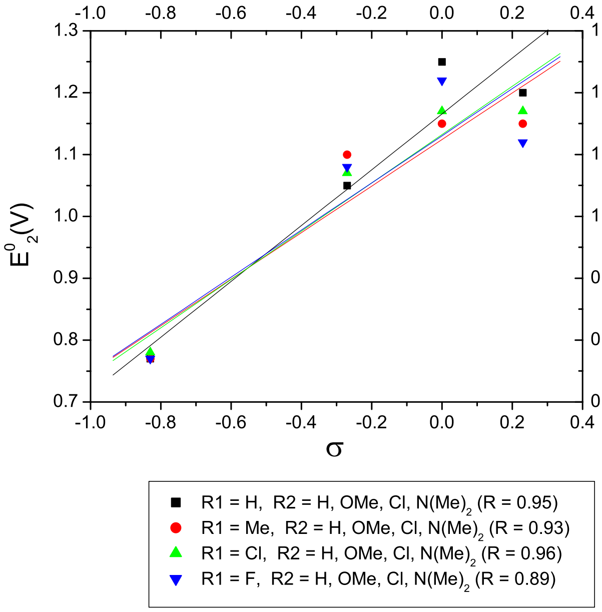

Fig. 7. Plot of E_0^2 (V) vs. Hammett substituents constant (σ) of R2 for a fixed R1.

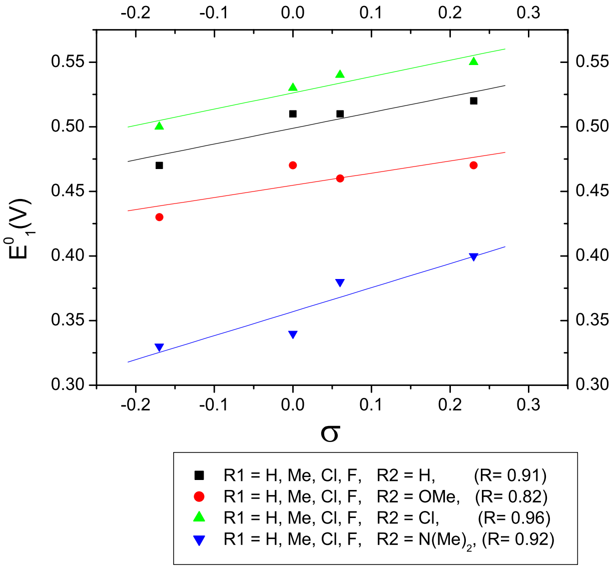

Fig. 8. Plot of E_0^1 (V) vs. Hammett substituents constant (σ) of R1 for a fixed R2.

matic rings of the ligands. Electron-donating substituents decreases, the redox potential and electron-withdrawing substituents increase the potential as expected. This is clearly revealed in the plots (Figs. 6–8) of E^0 values versus Hammett substituents constant (σ) of R1 and R2. Plots of the E_0^1 versus the energy of the HOMO of the molecules are also found to be approximately linear (Fig. 9), indicating that by suitable substitution in the R1 and R2 positions one can fine tune the HOMO energy over a range of 0.6 eV and the redox potential over a range of 0.2 V. The corresponding plot for E_0^2 is also linear, though the

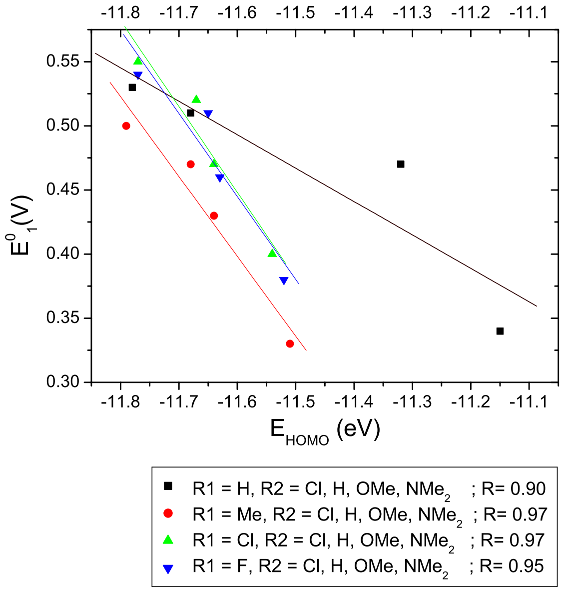

Fig. 9. Plot E_0^1 (V) versus energy of the HOMO of the metal complexes.

regression coefficient is much less satisfactory than that for E_0^1.

4. Conclusion

Study of 16 Ru(II) complexes of 1-(arylidine) 4-(aryl) thiosemicarbazones reported in this paper reveals that the structural parameters (e.g., Ru–N and Ru–P bond distances) and the oxidation potentials of these complexes can be fine tuned by changing the substitution in the 4-aryl (R1) as well as arylidine (R2) part. As expected the sensitivity towards variation at R2 is more than that at R1. A DFT calculation shows that the HOMO along with HOMO − 1 and HOMO − 2 orbitals has substantial contribution from the sulfur orbitals. Thus, assignment of the oxidation state of the metal ion in the oxidized form of these complexes must be made with caution unless supplemented with theoretical calculations or detailed spectroscopic characterization of the oxidized species.

Acknowledgments

D.M. and S.N. acknowledge CSIR and UGC, respectively, for their fellowships. S.K.C. acknowledges AICTE and UGC, New Delhi, for financial support. We thank EPSRC (UK) and the University of Reading for funds for the Image Plate System. We also acknowledge the use of UV–Vis spectrophotometer purchased from a DST (India)-FIST grant.

Appendix A. Supplementary data

Supplementary data associated with this article can be found, in the online version, at doi:10.1016/j.ica.2005.11.001.

References

[1] M.J.M. Campbell, Coord. Chem. Rev. 15 (1975) 297.

[2] D.X. West, S.B. Padhye, P.B. Sonawane, Struct. Bond. (Berlin) 76 (1991) 1.

[3] S.B. Padhye, G.B. Kauffman, Coord. Chem. Rev. 63 (1985) 127.

[4] D.X. West, A.E. Liberta, S.B. Padhye, R.C. Chikate, P.B. Sonawane, A.S. Kumbhar, R.G. Yerande, Coord. Chem. Rev. 123 (1993) 49.

[5] Y.P. Tian, C.Y. Duan, Z.L. Lu, X.Z. You, H.K. Fun, S. Kandasamy, Polyhedron 15 (1996) 2263.

[6] D.L. Klayman, J.P. Scovill, J.F. Bartosevich, J. Bruce, J. Med. Chem. 26 (1983) 39.

[7] D. Kovala-Demertzi, M.A. Demertzis, J.R. Miller, C. Padadopoulou, C. Dodorou, G. Filousis, J. Inorg. Biochem. 86 (2001) 555.

[8] A.G. Quiroga, J.M. Pérez, L-. Solera, J.R. Masaguer, A. Luque, P. Román, A. Edwards, C. Alonso, C.N-. Ranninger, J. Med. Chem. 41 (1998) 1399.

[9] D.H. Petering, Bioinorg. Chem. 1 (1972) 255.

[10] D. Kovala-Demertzi, A. Domopoulou, M.A. Demertzis, G. Valle, A. Papageorgiou, J. Inorg. Biochem. 68 (1997) 147.

[11] D. Kovala-Demertzi, P.N. Yadav, M.A. Demertzis, M. Coluccia, J. Inorg. Biochem. 78 (2000) 347.

[12] D.T. Minkel, D.H. Petering, Cancer Res. 38 (1978) 117.

[13] S.K. Chattopadhyay, S. Ghosh, Inorg. Chim. Acta 131 (1987) 15.

[14] S.K. Chattopadhyay, S. Ghosh, Inorg. Chim. Acta 163 (1989) 245.

[15] M. Maji, S. Ghosh, S.K. Chattopadhyay, T.C.W. Mak, Inorg. Chem. 36 (1997) 2938.

[16] F. Basuli, S.–M. Peng, S. Bhattacharya, Inorg. Chem. 36 (1997) 5645.

[17] F. Basuli, M. Ruf, C.G. Pierpont, S. Bhattacharya, Inorg. Chem. 37 (1998) 6113.

[18] F. Basuli, S.-M. Peng, S. Bhattacharya, Inorg. Chem. 39 (2000) 1120.

[19] P. Sengupta, R. Dinda, S. Ghosh, W.S. Sheldrick, Polyhedron 22 (2003) 447.

[20] S.K. Chattopadhyay, M. Hossain, S. Ghosh, A.K. Guha, Transition Met. Chem. 15 (1990) 473.

[21] F. Bregant, S. Pacor, S. Ghosh, S.K. Chattopadhyay, G. Sava, Anticancer Res. 13 (1993) 1007.

[22] P. Sengupta, S. Ghosh, T.C.W. Mak, Polyhedron 20 (2001) 975.

[23] P. Sengupta, R. Dinda, S. Ghosh, A.K. Guha, Transition Met. Chem. 27 (2002) 290.

[24] T.A. Stephenson, G. Wilkinson, J. Inorg. Nucl. Chem. 28 (1966) 945.

[25] D. Mishra, S. Naskar, R.J. Butcher, S.K. Chattopadhyay, Inorg. Chim. Acta 358 (2005) 3115.

[26] D. Mishra, S. Naskar, M.G.B. Drew, S.K. Chattopadhyay, Polyhedron 24 (2005) 1861.

[27] Hyperchem for Windows, Release 7.01, Hypercube Inc., 115 NW 4th Street, Gainesville, FL 32601, USA.

[28] ADF program, E.J. Baerends, A. Berces, C. Bo, P.M. Boerrigter, L. Cavallo, L. Deng, R.M. Dickson, D.E. Ellis, L. Fan, T.H. Fisher, C. Fonseca-Guerra, S.J.A. van Gisbergen, J.A. Groeneveld, O.V. Gritsenko, F.E. Harris, D. van Hoek, P.H. Jacobson, G. van Kessel, F. Kootstra, E. van Lenthe, V.E. Osinga, P.H.T. Philipson, D. Post. C.C. Pye, W. Ravenek, P. Ros, P.R.T. Schipper, G. Schreckenback, J.G. Snijders, M. Sola, D. Swerhone, G. te Velde, P. Vernooijs, L. Versluis, O. Visser, E. van Wezenbeek, G. Wiesenekker, S.K. Wolff, T. Woo, T. Ziegler, SCM Inc, Vrije Universiteit, Theoretical Chemistry, Amsterdam, The Netherlands, 2000.

[29] S.H. Vosko, L. Wilk, M. Nusair, Can. J. Phys. 58 (1980) 1200.

[30] A.D. Becke, J. Chem. Phys. 88 (1988) 1053.

[31] (a) J.P. Perdew, Phys. Rev. B 33 (1986) 8822;
(b) J.P. Perdew, Phys. Rev. B 34 (1986) 7406.

[32] W. Kabsch, J. Appl. Cryst. 21 (1988) 916.

[33] G.M. Sheldrick, Acta Cryst. A 46 (1990) 467.

[34] N. Walker, D. Stuart, Acta Cryst. A 39 (1983) 158.

[35] G.M. Sheldrick, Program for Crystal Structure Refinement, University of Gottingen, Gottingen, 1997.

[36] M.A. Greaney, C.L. Coyle, M.A. Harmer, A. Jordan, E.I. Stiefel, Inorg. Chem. 28 (1989) 912.

[37] M.-a. Haga, E.S. Dodsworth, A.B.P. Lever, Inorg. Chem. 25 (1986) 447.

[38] E.S. Dodsworth, A.B.P. Lever, Chem. Phys. Lett. 124 (1986) 152.